Published in final edited form as:
J Bioenerg Biomembr. 2014 February ; 46(1): 33–44. doi:10.1007/s10863-013-9530-z.

Dietary fat, fatty acid saturation and mitochondrial bioenergetics

Liping Yu[1], **Brian D. Fink**[2], **Judith A. Herlein**[2], **Christine L. Oltman**[3], **Kathryn G. Lamping**[4], and **William I. Sivitz**[2]

[1]NMR Core Facility and Department of Biochemistry, University of Iowa and the Iowa City Veterans Affairs Medical Center, Iowa City, IA, 52242

[2]Department of Internal Medicine/Endocrinology, University of Iowa and the Iowa City Veterans Affairs Medical Center, Iowa City, IA, 52242

[3]Department of Internal Medicine/Cardiology, University of Iowa and the Iowa City Veterans Affairs Medical Center, Iowa City, IA, 52242

[4]Department of Pharmacology, University of Iowa and the Iowa City Veterans Affairs Medical Center, Iowa City, IA, 52242

Abstract

Fat intake alters mitochondrial lipid composition which can affect function. We used novel methodology to assess bioenergetics, including simultaneous ATP and reactive oxygen species (ROS) production, in liver and heart mitochondria of C57BL/6 mice fed diets of variant fatty acid content and saturation. Our methodology allowed us to clamp ADP concentration and membrane potential ($\Delta\Psi$) at fixed levels. Mice received a control diet for 17–19 weeks, a high-fat (HF) diet (60% lard) for 17–19 weeks, or HF for 12 weeks followed by 6–7 weeks of HF with 50% of fat as menhaden oil (MO) which is rich in *n-3* fatty acids. ATP production was determined as conversion of 2-deoxyglucose to 2-deoxyglucose phosphate by NMR spectroscopy. Respiration and ATP production were significantly reduced at all levels of ADP and resultant clamped $\Delta\Psi$ in liver mitochondria from mice fed HF compared to controls. At given $\Delta\Psi$, ROS production per mg mitochondrial protein, per unit respiration, or per ATP generated were greater for liver mitochondria of HF-fed mice compared to control or MO-fed mice. Moreover, these ROS metrics began to increase at a lower $\Delta\Psi$ threshold. Similar, but less marked, changes were observed in heart mitochondria of HF-fed mice compared to controls. No changes in mitochondrial bioenergetics were observed in studies of separate mice fed HF versus control for only 12 weeks. In summary, HF feeding of sufficient duration impairs mitochondrial bioenergetics and is associated with a greater ROS "cost" of ATP production compared to controls. These effects are, in part, mitigated by MO.

Keywords

Mitochondria; ATP; Reactive Oxygen; Fatty Acids; Respiration

INTRODUCTION

Differences in dietary fat content and fatty acid saturation impact the structure of lipid bilayers including those comprising mitochondrial membranes (1, 2). Other consequences include perturbations in mitochondrial membrane fluidity (3), function of transporters (4),

Corresponding author: Dr. William Sivitz, Department of Internal Medicine, Division of Endocrinology and Metabolism, The University of Iowa Hospitals and Clinics, 422GH, 200 Hawkins Drive, Iowa City, IA. 52242., Phone: (319) 353-7812; Fax: (319) 353-7850, william-sivitz@uiowa.edu.

calcium dynamics (5, 6), gene expression (7), and post translational protein modifications (8). Hence, it is not surprising that mitochondrial function and production of reactive oxygen species (ROS) should be affected by dietary fat intake.

High dietary fat intake is associated with increased ROS production, decreased respiration, respiratory uncoupling, and reduced ATP production (9–12). However, the effects of the composition of dietary fat on mitochondrial function and ROS production are controversial. Dietary *n-3* fatty acids have been reported to reduce (13, 14) or enhance (15, 16) ROS production. Moreover, *n-3* fatty acids have been variably reported to inhibit or enhance respiration, respiratory uncoupling, and respiratory control ratios (13, 14, 17–19). These reported discrepancies could be due to different experimental conditions which affect the respiratory state causing variation between states 4 and 3. This variability can profoundly affect membrane potential, ROS levels, and other bioenergetic parameters.

Here we used new methodology to test the hypothesis that dietary saturated fat and/or substitution with *n-3* polyunsaturated fatty acids alters liver and heart mitochondrial function over a broad range of fixed respiratory states. To accomplish this, we employed a novel technique that we recently described (20) to assess ATP production in a highly sensitive and specific fashion under conditions of clamped mitochondrial inner membrane potential and in a way that enabled simultaneous measurement of ROS and ATP production. Our results shed new light on existing controversy regarding the relative effects of fat saturation on mitochondrial bioenergetics.

METHODS

Materials

Reagents were purchased as indicated or from standard sources.

Animal studies

Male C57BL/6 mice (age 12 weeks) were obtained from Jackson Laboratories (Bar Harbor, ME). Mice were fed a normal rodent diet (13% kcal fat, diet 7001, Teklad, Harlan Labs, Madison, WI) until initiation of the dietary protocol and maintained according to NIH guidelines. The protocol was approved by our institutional Animal Care Committee.

Two experimental protocols were carried out. The first (protocol I experiments) consisted of mice continued on the normal rodent diet described above (controls) or fed HF (lard, 60% kcal fat, D12492, Research Diets, New Brunswick, NJ). Mice were sacrificed after 12 weeks on these diet regimens. The second protocol (protocol II experiments) consisted of mice fed one of three different diet regimens. In two of the regimens mice were fed HF for 12 weeks. This was followed by another approximately 6 week period during which mice were either continued on the same HF diet or switched from the HF diet to a diet wherein 50% of the fat was provided as menhaden oil rich in *n-3* rich fatty acids (MO diet, *n-3* PUFA, D10122003, Research Diets, New Brunswick, NJ,). The third diet regimen consisted of mice fed the control normal rodent diet for the approximate 18 week period during which time the HF or MO mice were on their respective regimens. Mice in both protocols I and II were euthanized with sodium pentobarbital (150 mg/kg IP) to obtain tissues for study.

Mice studied in protocol II were utilized in a previously published study (21) designed to assess whole body glucose tolerance, gracilis muscle insulin signaling, and vascular reactivity of isolated gracilis muscle arteries. These parameters were impaired by HF feeding compared to control mice but improved in mice wherein HF (lard) was partially substituted by MO.

The energy density and nutrient and fatty acid composition of the dietary regimens are detailed in the online resource tables 1 and 2.

Whole animal gas exchange

O_2 consumption and CO_2 production were determined using a PhysioScan Metabolic System to assess gas exchange in small animals.

Isolation of mitochondria

Mitochondria were isolated as we previously described (22, 23). Mitochondrial protein was determined on homogenates of mitochondrial suspensions by the Bradford technique (Bio-Rad, Inc., Hercules, CA). Mitochondria prepared in this fashion were highly pure as indicated by the distribution of glyceraldehyde-3-phosphate dehydrogenase and porin in whole tissue and mitochondrial extracts (22). Mitochondrial integrity was assessed by cytochrome C release using a commercial kit (Cytochrome c Oxidase Assay Kit, Sigma-Aldrich, St. Louis) indicating over 90% intact mitochondria, well within an acceptable range compared to mitochondrial preparations from several sources (24).

Mitochondrial fatty acid composition and unsaturation indices

Fatty acid composition and unsaturation indices were determined on mitochondria obtained from the protocol II mice by gas-liquid chromatography (21). Mitochondrial lipids were extracted with a 2:1 (vol/vol) mixture of chloroform and methanol followed by phase separation with a solution of 154 mM NaCl and 4 mM HCl. Fatty acid composition was measured after the lipid fraction was transesterified in 14% boron trifluoride in methanol and the fatty acid methyl esters extracted into heptane before separation by gas-liquid chromatography. Individual fatty acid peaks as percent of total fatty acids were identified by comparison to known fatty acid standards. Unsaturation indices were calculated as the sum of (percent of each constituent fatty acid×number of double bonds in each fatty acid) divided by 100.

Respiration and membrane potential

Respiration and $\Delta\Psi$ were determined as we previously described (10, 23) using a 600 μl respiratory chamber fitted with an O_2 and potential sensitive tetraphenylphosphonium (TPP^+) electrode. Mitochondria (0.5 mg/ml for liver or 0.25 mg/ml for heart) were incubated in ionic respiratory buffer (120 mM KCl, 5 mM KH_2PO_4, 2 mM $MgCl_2$, 1 mM EGTA, 3 mM HEPES, pH 7.2 with 0.3% fatty acid free BSA). Mitochondria were fueled by combined substrates consisting of 5 mM succinate + 5 mM glutamate + 1 mM malate.

Generation of the 2-deoxyglucose ATP energy clamp

As we recently described (20), bioenergetic studies of heart and liver mitochondria were carried out in the presence of excess 2-deoxyglucose (2DOG) and hexokinase (HK) and varying amounts of added ADP or ATP. ATP added or generated from ADP under these conditions drives the conversion of 2DOG to 2DOG phosphate (2DOGP). The reaction occurs rapidly and irreversibly, thereby effectively clamping ADP concentrations and, consequently, also clamping $\Delta\Psi$ dependent on the amount of exogenous ADP or ATP added. The method, as we recently published (20), is depicted graphically (online resource figure 1). This technique enabled bioenergetic studies to be carried out over respiratory states ranging from state 4 (no added ADP) through states ranging from 4 to 3 (ADP added in different amounts). For this method to be effective membrane potential should decrease in stepwise fashion to plateau levels with each incremental addition of ADP (or ATP). Indeed, this was the case, as shown in figure 1. Likewise, plateau levels were achieved when incremental amounts of ATP, rather than ADP, were added (data not shown).

Use of the 2DOG ATP energy clamp to quantify ATP production in isolated mitochondria and simultaneous assessment of H_2O_2 production

Mitochondria (0.5 mg/ml for liver or 0.1 mg/ml for heart) were added to individual wells of 96-well plates in a total volume of 60 μl and incubated at 37°C in respiratory buffer plus 5 units/ml HK (Worthington Biochemical) and 5 mM 2DOG in the presence of selected concentrations of ADP and fueled by the combined substrates, 5 mM succinate + 5 mM glutamate + 1 mM malate. After incubation for 20 min, the contents of the microplate wells were removed to tubes on ice containing 1μl of 120 μM oligomycin to inhibit ATP synthase. Tubes were then centrifuged for 4 minutes at 14,000 × g to pellet the mitochondria. Supernatants were transferred to new tubes and stored at −20 °C until NMR analysis. To prepare the NMR sample, 40 μl of assay supernatant was added to a 5 mm (OD) standard NMR tube (Norell, Inc.) along with 50 μl of deuterium oxide (D_2O) and 390 μl of a buffer consisting of 120 mM KCl, 5 mM KH_2PO_4 and 2 mM $MgCl_2$, pH 7.2.

ATP production rates were calculated based on the percent conversion of 2DOG to 2DOGP, the initial 2DOG concentration, incubation volume, and incubation time. In order to simultaneously assess H_2O_2 production, mitochondrial incubations were carried out in the presence of 10-acetyl-3,7-dihydroxyphenoxazine as described below.

NMR spectroscopy

NMR spectra were collected at 37 °C on a Bruker Avance II 500 MHz NMR spectrometer. The 2DOG and 2DOGP ^1H and ^{13}C NMR resonances were assigned through ^1H homonuclear two-dimensional (2D) DQF-COSY (25) and TOCSY (26, 27) experiments and $^1H/^{13}C$ 2D heteronuclear multiple quantum coherence (HMQC) and heteronuclear multiple bond coherence (HMBC) experiments (28). Mitochondrial samples were studied by NMR spectroscopy by acquiring one-dimensional (1D) ^1H NMR spectra using unlabeled 2DOG in a NMR buffer containing 120 mM KCl, 5 mM KH_2PO_4, 2 mM $MgCl_2$, pH 7.2, 90%H_2O/10%D_2O as we recently described (20). The amount of 2DOG and 2DOGP present in the NMR samples were quantitatively measured using the peak intensities of the assigned resonances of these compounds. The ^1H chemical shifts are referenced to 2,2-dimethyl-2-silapentane-5-sulfonate (DSS). NMR spectra were processed with the NMRPipe package (29) and analyzed using NMRView software (30).

Mitochondrial ROS production

H_2O_2 production was assessed simultaneously with ATP production using the fluorescent probe 10-acetyl-3,7-dihydroxyphenoxazine (DHPA or Amplex Red, Invitrogen), a highly sensitive and stable substrate for horseradish peroxidase and a well-established probe for isolated mitochondria (31). Fluorescence was measured and quantification carried out as we previously described (23). Addition of catalase, 500 units/ml, reduced fluorescence to below the detectable limit, indicating specificity for H_2O_2. Addition of substrates to respiratory buffer without mitochondria did not affect fluorescence. DHPA does not interfere with ATP production or with NMR detection of 2DOGP (20).

Statistics

Data were analyzed by unpaired, two-tailed t-test or one-way ANOVA as indicated in the figure legends or text. Statistical analyses, calculations for area under the curve, and linear curve fitting and curve comparisons were performed using GraphPad Prism (GraphPad Software, Inc). Rates of respiration and ATP and H_2O_2 production (± SE) are expressed per mg mitochondrial protein or otherwise as described in the figure legends or text.

RESULTS

Mouse characteristics

Times of treatment and body weights for mice in both experimental protocols are listed in table 1. Other characteristics of the control, HF, and MO-treated mice were previously reported (21). HF-fed mice had higher fasting glucose and glucose tolerance in spite of about five-fold greater fasting insulin and leptin concentrations. These changes were partially mitigated in the MO mice wherein fasting glucose and glucose tolerance approached control levels while insulin concentrations were increased only 2–3 fold and leptin by only 3–4 fold. Our previous report (21) also showed that the HF mice had markedly increased liver fat on oil red O staining and that this effect was mitigated in the MO group.

Whole body respiration

The amount of O_2 consumed (VO_2) and CO_2 produced (VCO_2) were both significantly lower in the HF-fed mice compared to control mice, but partially mitigated in mice switched to MO (figure 2). Both the HF and MO groups tended to have a lower respiratory quotient (VCO_2/VO_2) compared to control mice, consistent with greater fat oxidation relative to glucose (although those values fell short of statistical significance).

Protocol I experiments

Mitochondrial function

No significant differences in respiration, potential, or ROS production were observed in protocol I experiments between the control and HF groups after 12 weeks of the dietary intervention (figure 3). Incremental amounts of ATP (for conversion to ADP) were added to determine respiration, potential, and ROS under energy clamped conditions. We observed no differences whether these parameters were assessed under state 4 conditions (no ATP added) or under conditions of clamped potential at fixed levels corresponding to respiratory states ranging from 4 to 3. As expected, heart mitochondria were metabolically more active than liver, manifest as greater oxygen consumption and higher ROS production.

Protocol II experiments—Protocol II experiments were carried out using ADP rather than ATP in the 2DOG energy clamp. This was done so that we could assess ATP production using the NMR technique. We had not completed the development and validation of this methodology (20) until after the protocol I studies were completed, so the ATP production assay was applied only to our protocol II studies.

Fatty acid composition and unsaturation indices

Fatty acid composition and unsaturation indices of mitochondrial lipids of control, HF, and MO-treated mice are depicted in the online resource table 3. Unsaturation indices were significantly greater in liver mitochondrial lipids of the MO-treated mice compared to those of control and HF-fed mice. Unsaturation indices were also significantly greater in heart mitochondrial lipids of the MO-treated mice compared to those of HF-fed mice and greater, but with missed significance, compared to controls.

Mitochondrial respiration

Respiration by liver mitochondria, assessed at different levels of clamped ADP (respiratory states ranging from state 4 to state 3), was reduced in HF-treated mice compared to control and to the mice switched to MO (figures 4A and 4B). Respiration was also plotted against clamped membrane potential resulting from the incremental levels of added ADP (figure 4C). This generated linear curves consistent with kinetic observations previously reported

for skeletal muscle mitochondria (32). The slopes were similar between groups. However, the regression line for the HF-fed mice was shifted to the left (lower respiration at given potential) compared to control and MO-fed mice.

Unlike liver mitochondria, oxygen consumption by heart mitochondria was not statistically different in the HF group compared to control or MO-treated mice. Nonetheless, a trend was evident in the same direction observed for liver mitochondria; i.e. lower oxygen consumption by the HF group at each increment in added ADP (figures 4D and 4E) and at each value for clamped potential (figure 4F).

ATP production

Generation of ATP was determined by conversion of 2DOG to 2DOGP under conditions of clamped ADP enabling assessment at respiratory states varying between 4 and 3 (figure 5). The mitochondria utilized were from the same preparations used to generate the data of figure 4 with the experiments run side by side in parallel fashion. ATP production by liver mitochondria of HF and MO-treated mice was reduced compared to control at all incremental levels of ADP (figures 5A and 5B). ATP production was also expressed as a function of clamped membrane potential resulting from the incremental ADP additions (figure 5C). These data showed that ATP synthesis by the HF-treated liver mitochondria was reduced relative to control at all clamped values of membrane potential and proceeded at lower $\Delta\Psi$.

Inspection of figure 5A shows that some ATP was produced even in the absence of added ADP (zero point), suggesting the presence of some endogenous ADP or ATP in these liver mitochondrial preparations. To determine whether endogenous ADP or ATP or both was present, we performed the mitochondrial incubations without added ADP but in the presence or absence of oligomycin. Generation of 2DOGP was observed only in the absence of oligomycin indicating the presence of endogenous ADP but not ATP in these samples (data not shown). The amount of endogenous ADP present would be low since subsequent addition of even 2.5 and 5 μM ADP substantially increased ATP production in all diet groups. Moreover, ATP production reached a plateau level at about 40 μM ADP for all diet groups.

ATP production by heart mitochondria of the HF-fed mice was reduced relative to the mitochondria from MO-fed mice (figures 5D and 5E). When expressed as a function of $\Delta\Psi$, ATP production by heart mitochondria of the HF-fed mice, similar to liver mitochondria, appeared to proceed at lower $\Delta\Psi$ compared to control or MO mice (figure 5F).

ROS production

H_2O_2 production was assessed as DHPA fluorescence simultaneously with ATP production (figure 5) and in parallel to the experiments measuring respiration and potential (figure 4). As expected, ROS production by liver mitochondria decreased markedly for all diet groups with progressively greater ADP concentrations and associated drop in $\Delta\Psi$ as respiration ranged from state 4 to state 3 (figures 6A and 6B). Absolute H_2O_2 production (H_2O_2 generated per mg mitochondrial protein) by liver mitochondria was greater for HF compared to MO and control mice (figure 6A). The difference between diet regimens became more evident when H_2O_2 production was plotted against the resulting clamped $\Delta\Psi$ (figure 6B) or when H_2O_2 production was expressed per unit oxygen consumption (figures 6C and 6D). Note that oxygen consumption is proportional to electron transport, i.e. the process wherein ROS are generated. HF-fed mice also generated more H_2O_2 per unit ATP produced (figures 6E and 6F), a biologic “cost” of oxidative phosphorylation.

Unlike liver mitochondria, absolute H_2O_2 production by heart mitochondria differed little between dietary treatment groups at any given ADP concentration (figure 7A). However, when absolute H_2O_2 production was plotted against the resulting $\Delta\Psi$ (figure 7B), it appeared that the $\Delta\Psi$ threshold for ROS production by the mitochondria from the HF mice was lower compared to mitochondria from the MO or control groups. Like liver mitochondria, this became more apparent when H_2O_2 was expressed relative to respiration (figures 7C and 7D) and when H_2O_2 was expressed per unit ATP produced (figures 7E and 7F).

DISCUSSION

We used a novel design and methodology to provide new bioenergetic data regarding mitochondrial function in mice fed diets differing in fatty acid content and saturation. Mice were initially fed control or HF diets followed by a change in fat composition in a portion of the mice. This approach more closely mimics what happens in overweight/obese humans who consume a high fat diet but at some point add dietary supplements or alter fat composition of their diet. Our studies are also novel in that we examined mitochondrial function and ROS production under clamped ADP and membrane potential. This differs from the conventional approach wherein the respiratory state is not precisely controlled since added ADP is consumed over time, during which potential decreases.

As we reported (20), there are several advantages to the ATP assay we employed, and these proved essential to our ability to carry out the current studies. In addition to the ability to clamp $\Delta\Psi$, the assay has sufficient sensitivity to measure ATP in small isolates of mitochondria, thereby enabling the study of samples from a single mitochondrial preparation under differing conditions. In fact, the 1D ^{1}H NMR method is 34-fold more sensitive compared to 1D ^{31}P NMR for ATP detection. Of note (although not applicable here) is that we have also implemented this assay in 2D mode showing that the $^{1}H/^{13}C$ HSQC NMR method is 41-fold more sensitive (20). Moreover, both the 1D and 2D NMR spectra are highly specific and there is good throughput since we can add mitochondria to multiple wells of a 96-well plate, incubate, spin off the mitochondria, and save the samples which can be directly used for NMR analysis. Finally, a very powerful aspect of this technique is that we can assess mitochondrial ROS production simultaneously with ATP formation since the ROS probe (DHPA) does not interfere with the NMR signals of interest and does not interfere with ATP production (20). We do note that the 2DOG clamp has been used in the past to assess mitochondrial-bound hexokinase activity at constant ADP (33). However, the technique has not been applied to ATP production or otherwise used as we have herein.

Our data show that HF impairs bioenergetics while *n-3* fatty acids as found in menhaden oil may offer benefits when substituted for saturated fat. Mice fed HF manifest reduced whole body oxygen consumption compared to controls (figure 2). Our data suggest that, at least for the protocol II mice, part of this can be explained at the mitochondrial level through lower respiration and workload energy (ATP production). Compared to mitochondria isolated from control and MO-fed mice, respiration ranging from state 4 to state 3 was significantly reduced in liver and trended lower in heart mitochondria from HF-fed mice (figures 4A, 4B, 4D, and 4E). Like respiration, ATP production was reduced in the liver and heart mitochondria from the HF-fed mice (figures 5A, 5B, 5D, and 5E). On the other hand, whole body respiration was reduced in the HF-fed mice of protocol I (figure 2B) even though the mitochondrial bioenergetics (figure 3) did not differ in protocol I. Of course whole body respiratory data may well diverge from findings in isolated mitochondria wherein the measured parameters represent intrinsic properties of the organelles *per se* and do not include cytoplasmic factors controlling metabolic flux. Moreover, respiratory changes could occur in tissues beyond liver and heart.

It has been suggested that respiratory uncoupling may explain how dietary regimens of different fatty acid saturation alter bioenergetics. Armstrong, et. al. (34) reported that *n-3* eicosapentaenoic acid, but not saturated fat, markedly upregulated UCP-2 mRNA expression in normal rat hepatocytes. In another study, Chen et. al.(13) found that a calorie restricted fish oil supplement diet compared to calorie restricted saturated fat increased the proton leak in heart mitochondria. However, our data are not consistent with uncoupling, at least not as the sole explanation for the bioenergetic differences between the MO and HF regimens. We did find greater respiration in the liver mitochondria of the MO mice compared to HF (figures 4A and 4B) which is compatible with relative uncoupling. However, ATP production at all levels of added ADP was very similar between the HF and MO groups (figures 5A and 5B) rather than reduced in the MO group, as would be expected for uncoupling. It is important to note that changes in UCP mRNA and even UCP protein expression do not consistently correspond to changes in proton leak (35) and that the changes in proton leak noted in the report of Chen et. al. (13) were in the context of calorie restriction; far different from the feeding experiments we carried out herein.

We can at least speculate that physical changes in mitochondrial membranes might explain the bioenergetic consequences of the dietary regimens we examined. As we observed here (online resource table 3) and as reported by others (2), dietary regimens rich in *n-3* fatty acids increase unsaturation indices in mitochondria and alter membrane lipid composition. This includes an increase in cardiolipin associated with increased respiration in heart (36) and increased ATP synthase activity in liver (37). Of note is that altered mitochondrial membrane lipid composition can alter membrane fluidity (3) and can change folding patterns that could alter proton flux and ATP synthase activity (38, 39).

The linearity of the relation between respiration and $\Delta\Psi$ created by clamped ADP levels (figures 4C and 4F) has been described before in studies of skeletal muscle wherein $\Delta\Psi$ was clamped using creatine phosphate and creatine kinase (32). This supports the proportionality of electron transport to the resultant driving force for oxidative phosphorylation, i.e. membrane potential.

High fat intake increases intracellular lipids associated with increased mitochondrial ROS (40, 41) and lipid peroxidation (9, 42). Our results are consistent showing that HF feeding increased liver mitochondrial ROS production compared to MO and control mice (figure 6). Although, it is known that PUFAs are more susceptible than saturated fatty acids to lipid peroxidation (1), our observation of lower ROS production by the MO mitochondria compared to HF is not inconsistent. The susceptibility of lipids to peroxidation results from hydrogen abstraction from a methylene group of a PUFA. So the presence of the site itself as well as the quantitative amount of ROS produced determines the extent of peroxidation.

Beyond quantification of ROS, our data show that production of ROS by liver mitochondria of the HF-fed mice was increased even as respiration proceeded towards state 3. Further, this increase occurred at a lower $\Delta\Psi$ threshold compared to control or MO-fed mice (figure 6B). This effect became more evident when ROS were expressed relative to electron transport (respiration) (figure 6D) or to the amount of ATP produced (figure 6F). For heart mitochondria ROS production for any given amount of clamped ADP did not differ significantly between mouse groups (figures 7A, 7C, and 7E). However, as in liver mitochondria, ROS generated by heart mitochondria from HF-fed mice increased at a lower $\Delta\Psi$ threshold relative to mitochondria from the MO or control mice (figure 7B). Again, this effect became more evident when ROS was expressed relative to respiration or ATP (figures 7D and 7F).

There is strong rationale for considering the metric “ROS production” not only in absolute terms but also, as we previously pointed out (43), per unit respiration (proportional to electron transport in isolated mitochondria). By analogy, comparing ROS generation between different experimental groups independent of electron transport is like comparing heat generated by different motor vehicle engines independent of speed. In fact, our current results indicate the importance of this. Our liver mitochondrial data (figure 6) showed that ROS per unit electron transport was enhanced to a greater extent than absolute ROS as a result of high fat feeding. In cardiac mitochondria, absolute ROS production appeared greater (although not significantly) in the MO group than the HF group (figures 7A and 7B). However, this was not the case when ROS was expressed per unit respiration.

With respect to the metric, “ROS per unit ATP”, this is significant in that it represents a biologic “cost” of oxidative phosphorylation; a factor of obvious interest when comparing physiologic states such as the dietary interventions examined herein. We also point out that the metrics “ROS per unit respiration” or “per unit ATP” produced are independent of mitochondrial mass since the units “mg protein” cancel in the numerator and denominator.

There are some limitations to our work. Studies of isolated mitochondria, as opposed to *in vivo* techniques such as phosphocreatine and ATP resynthesis and ATP saturation transfer (44), do not consider the external environment. However, isolated mitochondria can also be viewed as the only way to assess intrinsic properties of mitochondria as affected by interventions, in this case dietary. Another limitation is that our ROS studies measured mitochondrial superoxide indirectly as H_2O_2. As measured in this work and many other studies, H_2O_2 represents superoxide generated via the electron transport chain after conversion to H_2O_2 by manganese superoxide dismutase and released external to mitochondria for DHPA fluorescent detection (23, 45). Conversely, DHPA fluorescence has become a widely accepted standard for ROS production by isolated mitochondria (46) and, with our methodology, was assessed simultaneously with ATP. Another limitation is that all studies were carried out in mitochondria fueled by combined substrates. This was done to assess bioenergetics under a continuous or “closed” TCA cycle. Finally, we point out that although the substitution of MO seemed to mitigate the effects of HF feeding when added from 12 to 18 weeks, further study will be needed to see if we can reverse the effects evident in the HF mice at 18 weeks.

In summary, high fat feeding is associated with reduced whole body respiration and, over sufficient duration, results in reduced mitochondrial respiration and ATP production. High fat feeding also results in more ROS per unit respiration and per unit ATP produced. These impaired HF-induced bioenergetics are, in part, mitigated by partial substitution of *n-3* fatty acids in the diet. We used novel methodology to demonstrate these effects over a broad range of fixed respiratory states and show that ROS production by mitochondria of HF-fed mice begins to increase at a lower $\Delta\Psi$ threshold.

Supplementary Material

Refer to Web version on PubMed Central for supplementary material.

Acknowledgments

These studies were supported by resources and the use of facilities at the Department of Veterans Affairs Iowa City Health Care System, Iowa City, IA 52246, by VA Merit Awards to Kathryn G. Lamping (BX000543-03), Christine L. Oltman (BX000857-01), and William I. Sivitz (BX000285), and by the Fraternal Order of the Eagles. The contents of this manuscript are the sole responsibility of the authors and do not necessarily represent the official views of the granting agencies. The authors have no conflicts of interest to report.

References

1. Al-Gubory KH. Mitochondria: omega-3 in the route of mitochondrial reactive oxygen species. Int J Biochem Cell Biol. 2012; 44:1569–1573. [PubMed: 22710344]
2. Rohrbach S. Effects of dietary polyunsaturated fatty acids on mitochondria. Curr Pharm Des. 2009; 15:4103–4116. [PubMed: 20041812]
3. Tsalouhidou S, Argyrou C, Theofilidis G, Karaoglanidis D, Orfanidou E, Nikolaidis MG, Petridou A, Mougios V. Mitochondrial phospholipids of rat skeletal muscle are less polyunsaturated than whole tissue phospholipids: implications for protection against oxidative stress. J Anim Sci. 2006; 84:2818–2825. [PubMed: 16971584]
4. Hoch FL. Cardiolipins and biomembrane function. Biochim Biophys Acta. 1992; 1113:71–133. [PubMed: 1550861]
5. Patergnani S, Suski JM, Agnoletto C, Bononi A, Bonora M, De Marchi E, Giorgi C, Marchi S, Missiroli S, Poletti F, Rimessi A, Duszynski J, Wieckowski MR, Pinton P. Calcium signaling around Mitochondria Associated Membranes (MAMs). Cell Commun Signal. 2011; 9:19. [PubMed: 21939514]
6. Pepe S, Tsuchiya N, Lakatta EG, Hansford RG. PUFA and aging modulate cardiac mitochondrial membrane lipid composition and Ca2+ activation of PDH. Am J Physiol. 1999; 276:H149–158. [PubMed: 9887028]
7. Flachs P, Horakova O, Brauner P, Rossmeisl M, Pecina P, Franssen-van Hal N, Ruzickova J, Sponarova J, Drahota Z, Vlcek C, Keijer J, Houstek J, Kopecky J. Polyunsaturated fatty acids of marine origin upregulate mitochondrial biogenesis and induce beta-oxidation in white fat. Diabetologia. 2005; 48:2365–2375. [PubMed: 16205884]
8. Hasselbaink DM, Roemen TH, van der Vusse GJ. Protein acylation in the cardiac muscle like cell line, H9c2. Mol Cell Biochem. 2002; 239:101–112. [PubMed: 12479575]
9. Boudina S, Sena S, Theobald H, Sheng X, Wright JJ, Hu XX, Aziz S, Johnson JI, Bugger H, Zaha VG, Abel ED. Mitochondrial energetics in the heart in obesity-related diabetes: direct evidence for increased uncoupled respiration and activation of uncoupling proteins. Diabetes. 2007; 56:2457–2466. [PubMed: 17623815]
10. Fink BD, Herlein JA, Almind K, Cinti S, Kahn CR, Sivitz WI. The mitochondrial proton leak in obesity-resistant and obesity-prone mice. Am J Physiol Regul Integr Comp Physiol. 2007; 293:R1773–1780. [PubMed: 17761507]
11. Pires KM, Ilkun O, Valente M, Boudina S. Treatment with a SOD Mimetic Reduces Visceral Adiposity, Adipocyte Death, and Adipose Tissue Inflammation in High Fat-Fed Mice. Obesity (Silver Spring). 2013
12. Wang HT, Liu CF, Tsai TH, Chen YL, Chang HW, Tsai CY, Leu S, Zhen YY, Chai HT, Chung SY, Chua S, Yen CH, Yip HK. Effect of obesity reduction on preservation of heart function and attenuation of left ventricular remodeling, oxidative stress and inflammation in obese mice. J TransI Med. 2012; 10:145.
13. Chen Y, Hagopian K, Bibus D, Villalba JM, Lopez-Lluch G, Navas P, Kim K, McDonald RB, Ramsey JJ. The influence of dietary lipid composition on liver mitochondria from mice following 1 month of calorie restriction. Biosci Rep. 2013; 33:83–95. [PubMed: 23098316]
14. Hagopian K, Weber KL, Hwee DT, Van Eenennaam AL, Lopez-Lluch G, Villalba JM, Buron I, Navas P, German JB, Watkins SM, Chen Y, Wei A, McDonald RB, Ramsey JJ. Complex l-associated hydrogen peroxide production is decreased and electron transport chain enzyme activities are altered in n-3 enriched fat-1 mice. PLoS One. 2010; 5:el2696.
15. Fukui M, Kang KS, Okada K, Zhu BT. EPA, an omega-3 fatty acid, induces apoptosis in human pancreatic cancer cells: role of ROS accumulation, caspase-8 activation, and autophagy induction. J Cell Biochem. 2013; 114:192–203. [PubMed: 22903547]
16. Kang KS, Wang P, Yamabe N, Fukui M, Jay T, Zhu BT. Docosahexaenoic acid induces apoptosis in MCF-7 cells in vitro and in vivo via reactive oxygen species formation and caspase 8 activation. PLoS One. 2010; 5:el0296.
17. Aoun M, Feillet-Coudray C, Fouret G, Chabi B, Crouzier D, Ferreri C, Chatgilialoglu C, Wrutniak-Cabello C, Cristol JP, Carbonneau MA, Coudray C. Rat liver mitochondrial membrane

characteristics and mitochondrial functions are more profoundly altered by dietary lipid quantity than by dietary lipid quality: effect of different nutritional lipid patterns. Br J Nutr. 2012; 107:647–659. [PubMed: 21774841]

18. Oliveira CP, Coelho AM, Barbeiro HV, Lima VM, Soriano F, Ribeiro C, Molan NA, Alves VA, Souza HP, Machado MC, Carrilho FJ. Liver mitochondrial dysfunction and oxidative stress in the pathogenesis of experimental nonalcoholic fatty liver disease. Braz J Med Biol Res. 2006; 39:189–194. [PubMed: 16470305]
19. Stillwell W, Jenski LJ, Crump FT, Ehringer W. Effect of docosahexaenoic acid on mouse mitochondrial membrane properties. Lipids. 1997; 32:497–506. [PubMed: 9168456]
20. Yu L, Fink BD, Herlein JA, Sivitz WI. Mitochondrial function in diabetes: novel methodology and new insight. Diabetes. 2013; 62:1833–1842. [PubMed: 23328129]
21. Lamping KG, Nuno DW, Coppey LJ, Holmes AJ, Hu S, Oitman CL, Norris AW, Yorek MA. Modification of high saturated fat diet with n-3 polyunsaturated fat improves glucose intolerance and vascular dysfunction. Diabetes Obes Metab. 2013; 15:144–152. [PubMed: 22950668]
22. Herlein JA, Fink BD, O'Malley Y, Sivitz WI. Superoxide and respiratory coupling in mitochondria of insulin-deficient diabetic rats. Endocrinology. 2009; 150:46–55. [PubMed: 18772240]
23. O'Malley Y, Fink BD, Ross NC, Prisinzano TE, Sivitz WI. Reactive oxygen and targeted antioxidant administration in endothelial cell mitochondria. J Biol Chem. 2006; 281:39766–39775. [PubMed: 17060316]
24. Wojtczak L, Zaluska H, Wroniszewska A, Wojtczak AB. Assay for the intactness of the outer membrane in isolated mitochondria. Acta Biochim Pol. 1972; 19:227–234. [PubMed: 4347175]
25. Rance M, Sørensen OW, Bodenhausen G, Wagner G, Ernst RR, Wüthrich K. Improved spectral resolution in COSY 1H NMR spectra of proteins via double quantum filtering. Biochem Biophys Res Commun. 1983; 117:479–485. [PubMed: 6661238]
26. Braunschweiler L, Ernst RR. Coherence transfer by isotropic mixing: Application to proton correlation spectroscopy. J Magn Reson. 1983; 53:521–528.
27. Bax A, Davis DG. MLEV-17-based two-dimensional homonuclear magnetization transfer spectroscopy. J Magn Reson. 1985; 65:355–360.
28. Nyberg NT, Sürensen OW. Multiplicity-edited broadband HMBC NMR spectra. Magn Reson Chem. 2006; 44:451–454. [PubMed: 16425209]
29. Delaglio F, Grzesiek S, Vuister GW, Zhu G, Pfeifer J, Bax A. NMRPipe: A multidimensional spectral processing system based on UNIX pipes. J Biomol NMR. 1995; 6:277–293. [PubMed: 8520220]
30. Johnson BA, Blevins RA. NMR View: A computer program for the visualization and analysis of NMR data. J Biomol NMR. 1994; 4:603–614. [PubMed: 22911360]
31. Rhee SG, Chang TS, Jeong W, Kang D. Methods for detection and measurement of hydrogen peroxide inside and outside of cells. Mol Cells. 2010; 29:539–549. [PubMed: 20526816]
32. Glancy B, Willis WT, Chess DJ, Balaban RS. Effect of calcium on the oxidative phosphorylation cascade in skeletal muscle mitochondria. Biochemistry. 2013; 52:2793–2809. [PubMed: 23547908]
33. da-Silva WS, Gomez-Puyou A, de Gomez-Puyou MT, Moreno-Sanchez R, De Felice FG, de Meis L, Oliveira MF, Galina A. Mitochondrial bound hexokinase activity as a preventive antioxidant defense: steady-state ADP formation as a regulatory mechanism of membrane potential and reactive oxygen species generation in mitochondria. J Biol Chem. 2004; 279:39846–39855. [PubMed: 15247300]
34. Armstrong MB, Towle HC. Polyunsaturated fatty acids stimulate hepatic UCP-2 expression via a PPARalpha-mediated pathway. Am J Physiol Endocrinol Metab. 2001; 281:E1197–1204. [PubMed: 11701434]
35. Cadenas S, Buckingham JA, Samec S, Seydoux J, Din N, Dulloo AG, Brand MD. UCP2 and UCP3 rise in starved rat skeletal muscle but mitochondrial proton conductance is unchanged. FEBS Letters. 1999; 462:257–260. [PubMed: 10622707]
36. McMillin JB, Bick RJ, Benedict CR. Influence of dietary fish oil on mitochondrial function and response to ischemia. Am J Physiol. 1992; 263:H1479–1485. [PubMed: 1332513]

37. Aoun M, Fouret G, Michel F, Bonafos B, Ramos J, Cristol JP, Carbonneau MA, Coudray C, Feillet-Coudray C. Dietary fatty acids modulate liver mitochondrial cardiolipin content and its fatty acid composition in rats with non alcoholic fatty liver disease. J Bioenerg Biomembr. 2012; 44:439–452. [PubMed: 22689144]
38. Johnson JA, Ogbi M. Targeting the FIFo ATP Synthase: modulation of the body's powerhouse and its implications for human disease. Curr Med Chem. 2011; 18:4684–4714. [PubMed: 21864274]
39. Strauss M, Hofhaus G, Schroder RR, Kuhlbrandt W. Dimer ribbons of ATP synthase shape the inner mitochondrial membrane. Embo J. 2008; 27:1154–1160. [PubMed: 18323778]
40. Brand MD, Esteves TC. Physiological functions of the mitochondrial uncoupling proteins UCP2 and UCP3. Cell Metabolism. 2005; 2:85–93. [PubMed: 16098826]
41. Yamagishi SI, Edelstein D, Du XL, Kaneda Y, Guzman M, Brownlee M. Leptin induces mitochondrial superoxide production and monocyte chemoattractant protein-1 expression in aortic endothelial cells by increasing fatty acid oxidation via protein kinase A. Journal of Biological Chemistry. 2001; 276:25096–25100. [PubMed: 11342529]
42. Pillon NJ, Croze ML, Vella RE, Soulere L, Lagarde M, Soulage CO. The lipid peroxidation by-product 4-hydroxy-2-nonenal (4-HNE) induces insulin resistance in skeletal muscle through both carbonyl and oxidative stress. Endocrinology. 2012; 153:2099–2111. [PubMed: 22396448]
43. Herlein JA, Fink BD, Henry DM, Yorek MA, Teesch LM, Sivitz WI. Mitochondrial superoxide and coenzyme Q in insulin-deficient rats: increased electron leak. Am J Physiol Regul Integr Comp Physiol. 2011; 301:R1616–1624. [PubMed: 21940403]
44. Szendroedi J, Phielix E, Roden M. The role of mitochondria in insulin resistance and type 2 diabetes mellitus. Nat Rev Endocrinol. 2012; 8:92–103. [PubMed: 21912398]
45. Lambert AJ, Brand MD. Inhibitors of the quinone-binding site allow rapid superoxide production from mitochondrial NADH:ubiquinone oxidoreductase (complex I). Journal of Biological Chemistry. 2004; 279:39414–39420. [PubMed: 15262965]
46. Brand MD. The sites and topology of mitochondrial superoxide production. Exp Gerontol. 2010; 45:466–472. [PubMed: 20064600]

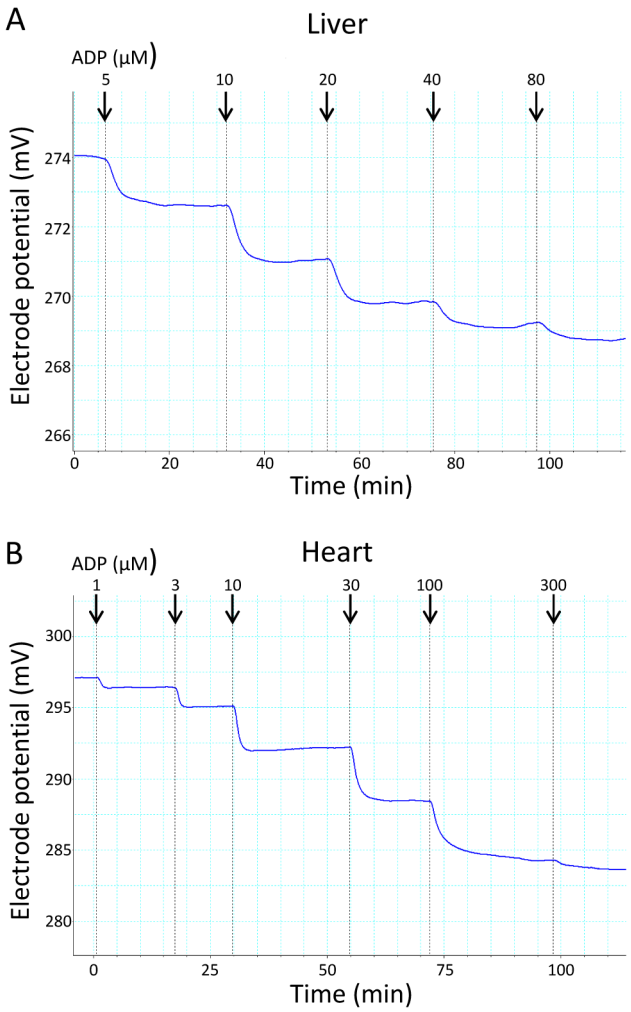

Figure 1.

Representative computer tracings of inner membrane potential vs. time obtained by incubating normal mouse liver mitochondria, 0.5 mg/ml, (panel A) or heart mitochondria, 0.25 mg/ml, (panel B) fueled by the combined substrates, 5 mM succinate + 5 mM glutamate + 1 mM malate. ADP was added in incremental amounts to generate the final total recycling nucleotide phosphate concentrations (indicated by arrows). After each addition, a plateau potential was reached, consistent with recycling at a steady ADP concentration and generation of a stepwise transition from state 4 to state 3 respiration. Note that the potential shown on the y-axis represents electrode potential (not mitochondrial potential). The actual $\Delta\Psi$ follows a similar pattern after calculation using the Nernst equation based on the distribution of tetraphenylphosphonium (TPP) external and internal to mitochondria.

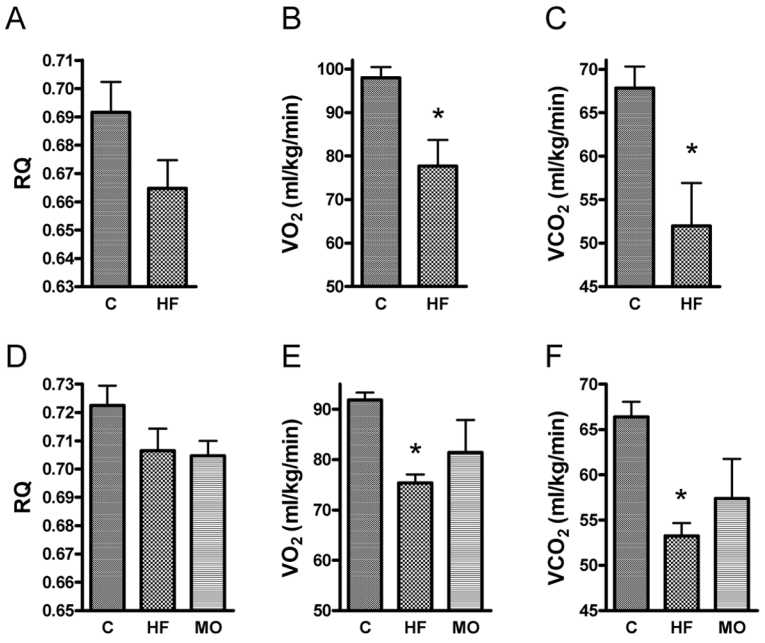

Figure 2.

Whole body respiratory parameters in mice fed control (C), high-fat (HF), or HF partially substituted with menhaden oil (MO) diets. Respiratory quotients (RQ), VO_2, and VCO_2 are shown for protocol I studies (panels A, B, and C, respectively) and protocol II studies (panels D, E, and F, respectively). Data represent mean ± SE, * $p < 0.05$ compared to control by unpaired, two-tailed t-test or one way ANOVA with Newman-Keuls multiple comparison test.

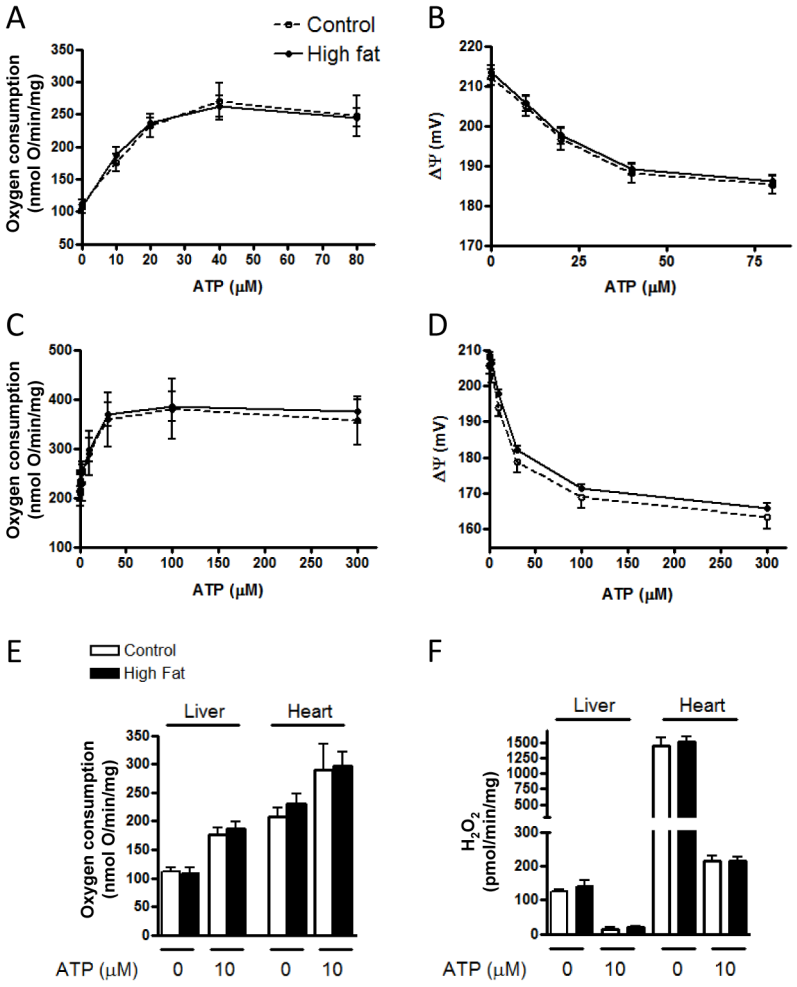

Figure 3.

Respiration, inner membrane potential, and ROS production by liver and heart mitochondria of protocol I mice treated with control or HF diets for 12 weeks. Oxygen consumption and membrane potential as a function of the amount of ATP added are shown for liver mitochondria (panels A and B) and for heart mitochondria (panels C and D), respectively. Oxygen consumption and H_2O_2 production at selected 0 and 10 μM ATP are shown for liver and heart mitochondria in panels E and F, respectively. No significant differences in respiration, potential, or ROS production by diet intervention were observed for either liver or heart mitochondria. “mg” in y-axis (panels A, C, E, F) refers to mg mitochondrial protein.

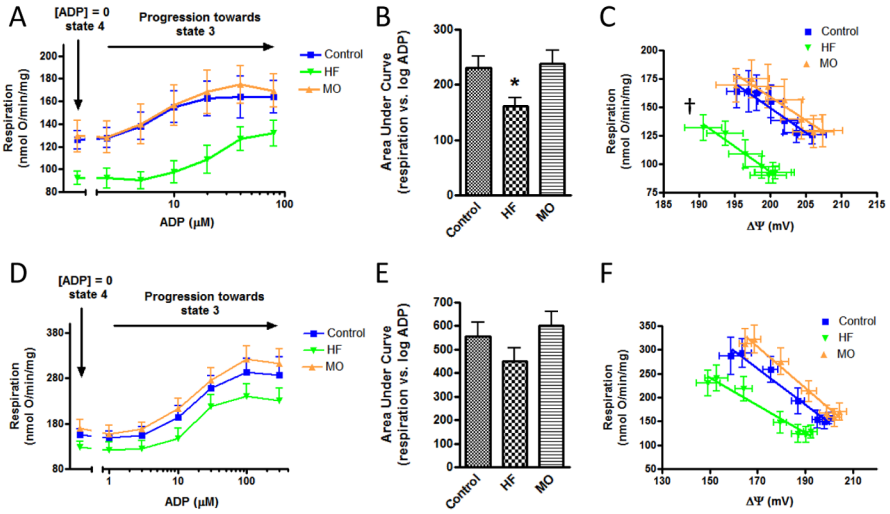

Figure 4.

Respiration by liver and heart mitochondria of protocol II mice at different levels of clamped ADP representing respiratory states ranging from state 4 to state 3. A) Respiration by liver mitochondria as a function of added ADP in control, high-fat (HF) or menhaden oil (MO) treated mice. B) Data of panel A compared as area under the curves. C) Respiration by liver mitochondria as a function of clamped inner membrane potential (ΔΨ) resulting from the incremental ADP concentrations of panel A. D–F) Data for heart mitochondria corresponding to the liver mitochondrial studies of panels A–C. * $p < 0.05$ compared to control and to MO by one-way ANOVA and Newman-Keuls multiple comparison test. † $p < 0.01$ for difference in curve elevation (HF versus MO or control). “mg” in y-axis (panels A, C, D, F) refers to mg mitochondrial protein.

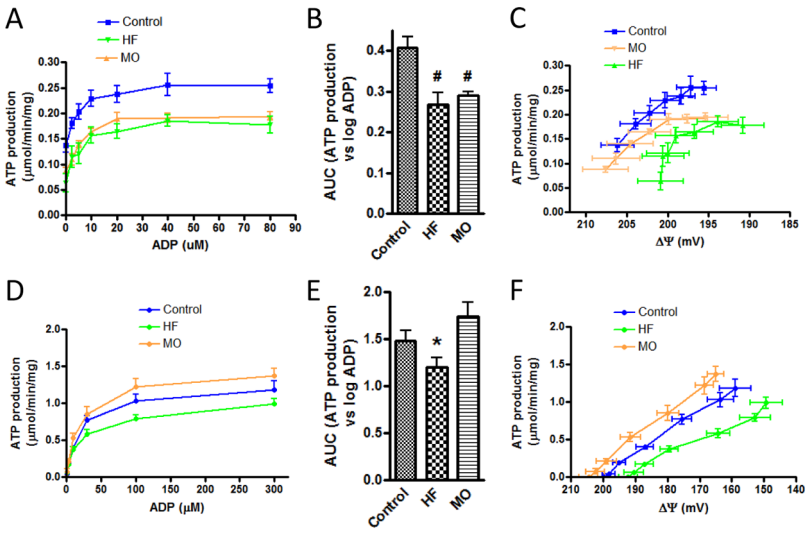

Figure 5.

ATP production by liver and heart mitochondria of protocol II mice at different levels of clamped ADP representing respiratory states ranging from state 4 to state 3. A) ATP production by liver mitochondria as a function of added ADP in control, high-fat (HF) or menhaden oil (MO) treated mice. B) Data of panel A compared as area under the curves (AUC). C) ATP production by liver mitochondria as a function of clamped inner membrane potential (ΔΨ) resulting from the incremental ADP concentrations of panel A. D–F) Data for heart mitochondria corresponding to the liver mitochondrial studies of panels A–C. # $p < 0.01$ compared to control and * $p < 0.05$ compared to MO by one-way ANOVA and Newman-Keuls multiple comparison test. “mg” in y-axis (panels A, C, D, F) refers to mg mitochondrial protein.

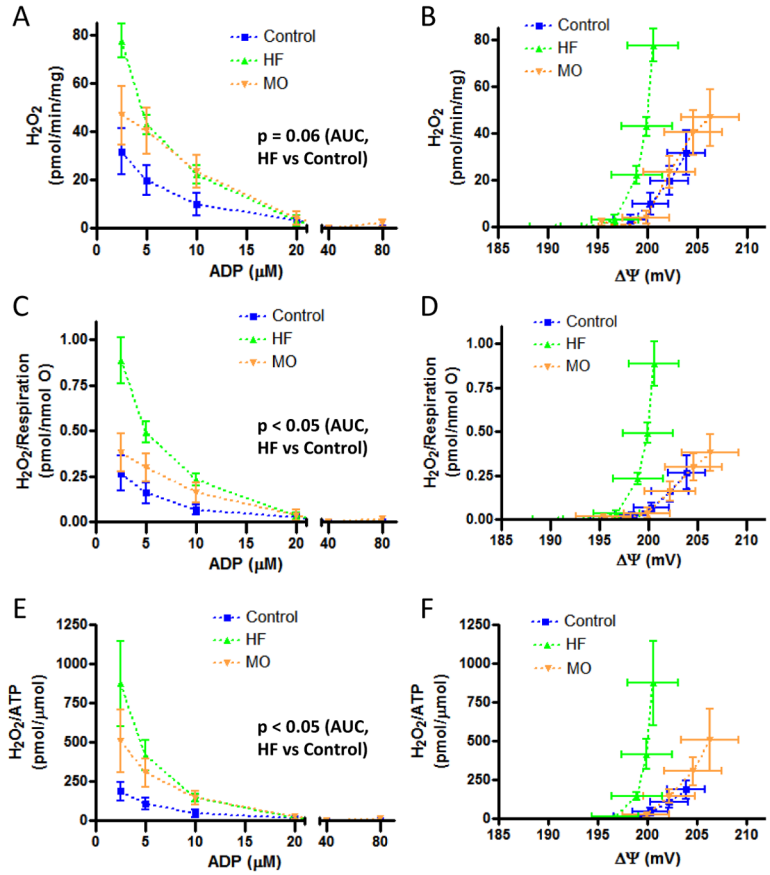

Figure 6.

H_2O_2 production by liver mitochondria of protocol II control, HF-fed, or MO-fed mice. A and B) Absolute values for H_2O_2 production as a function of ADP added to the medium (panel A) and resultant clamped ΔΨ (panel B). C and D) H_2O_2 production expressed per unit respiration as a function of added ADP (panel C) and resultant clamped ΔΨ (panel D). E and F) H_2O_2 production expressed per unit ATP generated as a function of added ADP (panel E) and resultant clamped ΔΨ (panel F). p values shown in panels A, C, and E represent the level of significance of differences in comparative values for area under the curve (AUC) by t-test with Bonferroni correction for multiple comparisons. Values at zero added ADP (near state 4 condition) are not shown since H_2O_2 production was 2–4 fold higher than at the lowest added ADP accounting for most of the AUC and obscuring the differences in the presence of added ADP (p-values did remain significant if the data at zero added ADP are included). “mg” in y-axis (panels A, B) refers to mg mitochondrial protein.

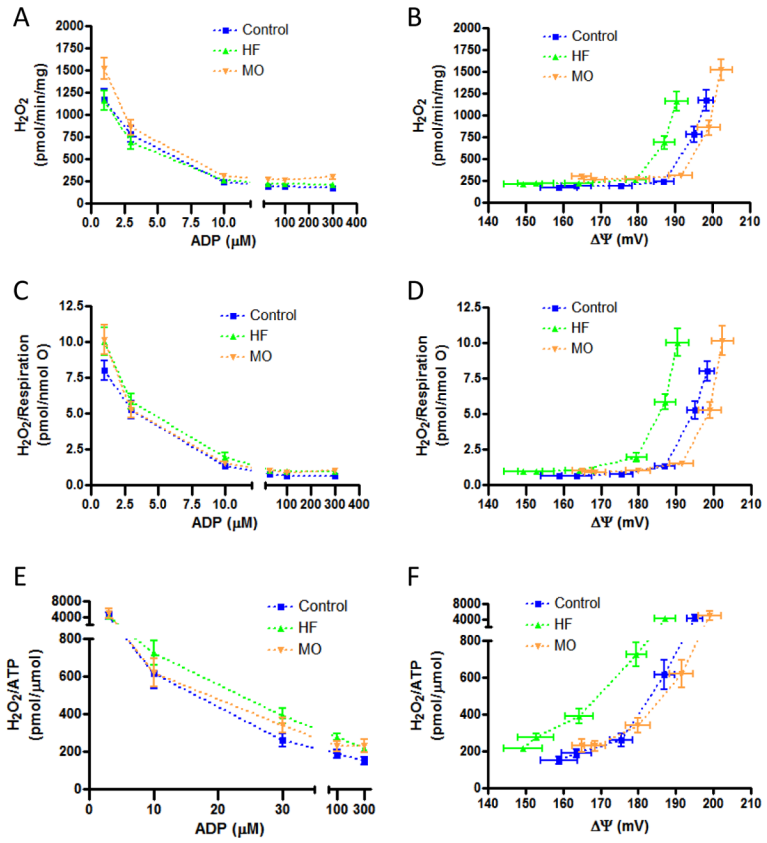

Figure 7.

H_2O_2 production by heart mitochondria of protocol II control, HF-fed, or MO-fed mice. A and B) Absolute values for H_2O_2 production as a function of ADP added to the medium (panel A) and resultant clamped ΔΨ (panel B). C and D) H_2O_2 production expressed per unit respiration as a function of added ADP (panel C) and resultant clamped ΔΨ (panel D). E and F) H_2O_2 production expressed per unit ATP generated as a function of added ADP (panel E) and resultant clamped ΔΨ (panel F). H_2O_2/ATP are not shown for the lowest ADP concentration since ATP production was very low and H_2O_2 very high (near state 4 conditions) leading to extreme variability in the ratio. Data did not differ significantly by statistical analyses as applied in figure 6. Values for all H_2O_2 metrics at zero added ADP are not shown for the reason indicated in the legend to figure 6. “mg” in y-axis (panels A, B) refers to mg mitochondrial protein.

Table 1

Characteristics of the mice in protocols I and II

	Initial Weight (g)	Age at onset of diet (days)	Number days treated	Weight gain (g)
Protocol I				
Control (n = 7)	29.0 ± 0.8	90	89.7 ± 1.4	5.0 ± 0.6
HF (n = 7)	25.9 ± 1.6	90	89.7 ± 1.4	18.2 ± 2.7 *
Protocol II				
Control (n = 5)	29.0 ± 0.5	90	124 ± 3	5.9 ± 1.3
HF (n = 6)	26.4 ± 0.5	90	128 ± 3	25.5 ± 1.3 *
MO (n = 6)	27.1 ± 1.0	90	131 ±2	21.3 ± 2.2 *

Data represent mean ± SE,

* $p < 0.001$ compared to control by unpaired, t-test (protocol I) or one-way ANOVA (protocol II).